Original Paper

Brain, Behavior and Evolution

Brain Behav Evol 2008;72:192–206
DOI: 10.1159/000157356

Received: June 16, 2007
Returned for revision: July 26, 2007
Accepted after second revision: June 19, 2008
Published online: September 25, 2008

Comparative Study of TPep-Like Immunoreactive Neurons in the Central Nervous System of Nudibranch Molluscs

Michael J. Baltzley Kenneth J. Lohmann

Department of Biology, University of North Carolina at Chapel Hill, Chapel Hill, N.C., USA

Key Words

Tritonia · Gastropods · Evolution · Pedal ganglion · TPeps · Nudibranchs · Mucociliary · Motor neurons · Invertebrates

Abstract

In the sea slug *Tritonia diomedea*, mucociliary crawling is controlled partly by two pairs of bilaterally symmetrical neurons located in the pedal ganglia. These neurons, known as the Pedal 5 and Pedal 6 cells, produce a class of neuropeptides called TPeps. Using immunohistochemistry we identified TPep-like immunoreactive (TPep-LIR) neurons in diverse nudibranch species. All species examined had 2–7 large, TPep-LIR cells located in each pedal ganglion. The absolute size of the largest TPep-LIR neuron was correlated with foot size. Species with a bigger foot size tended to have larger TPep-LIR cells. However, the number of cells in a given species was not correlated with the size of the adult foot. The presence of large, TPep-LIR cells across the nudibranchs suggests that part of the neural circuitry controlling mucociliary locomotion has been conserved, although the size and number of cells is variable across species. We conclude that the motor circuit underlying crawling might adapt to changes in foot size by changing the size of motor neurons in the circuit, but that changes in cell number are not directly related to foot size.

Introduction

In the search for general principles of how evolution shapes neural circuits, a fundamental issue is identifying which elements of nervous systems tend to be conserved and which elements are evolutionarily labile [Croll, 1987; Breidbach and Kutsch, 1995]. One strategy for identifying evolutionarily labile traits in the nervous system is to look for variation in closely related species. Ideally, this nervous system variation can be correlated with behavioral and morphological traits to help understand how the nervous system evolves in response to selection on behavioral or morphological phenotypes [Paul, 1991]. In this study, we examined part of the neural circuitry that controls crawling in the nudibranch gastropods, or sea slugs, and looked for correlations between neuroanatomy and foot size.

Whereas most slugs and snails crawl using muscular waves, the nudibranchs crawl using mucociliary locomotion [Agersborg, 1922, 1923; Audesirk, 1978; Crow and Tian, 2003]. Mucociliary crawling in the sea slug *Tritonia diomedea* is controlled in part by the bilaterally symmetrical Pedal 5 (Pd5) and Pedal 6 (Pd6) cells. The Pd5 and Pd6 cells cause an increase in the ciliary beat frequency at the pedal epithelium and thereby increase crawling speed [Willows et al., 1997; Popescu and Frost, 2002;

KARGER

Fax +41 61 306 12 34
E-Mail karger@karger.ch
www.karger.com

Accessible online at:
www.karger.com/bbe

Michael J. Baltzley
St. Mary's College of Maryland
Department of Biology, 18952 E. Fisher Road
St. Mary's City, MD 20686-3001 (USA)
Tel. +1 619 818 3868, Fax +1 240 895 4996, E-Mail mjbaltzley@smcm.edu

Wang et al., 2003]. Anatomical findings suggest that the Pd5 cells innervate the entire foot and the Pd6 cells innervate the anterior end of the foot [Popescu and Willows, 1999; Wang et al., 2003; Cain et al., 2006].

The Pd5 and Pd6 cells are easily identifiable in *T. diomedea* because of their size and location [Willows et al., 1973]. The cells are large, up to 500 μm in diameter, and are located on the dorsal surface of the pedal ganglia. The Pd5 and Pd6 cells are also identified by the presence of the neuropeptides TPeps [Lloyd et al., 1996; Beck et al., 2000]. TPeps cause an increase in ciliary beating when applied to isolated patches of the ciliated pedal epithelium and when applied to isolated ciliated cells [Willows et al., 1997]. TPep-like immunoreactive (TPep-LIR) cells of a similar size and location to the *T. diomedea* Pd5 and Pd6 cells have been identified in the central ganglia of the nudibranch *Phestilla sibogae* [Croll et al., 2001]. In this study, we examined 11 additional species of nudibranchs for the presence of similar TPep-LIR cells.

A common finding in comparative neuroanatomical studies is that cell types are conserved but the number of cells of a given type are variable [Paul, 1991; Turrigiano and Selverston, 1991; Witten and Truman, 1998; Katz and Harris-Warrick, 1999; Tierney et al., 1999; Page and Parries, 2000; Katz et al., 2001; Page, 2002; Espinoza et al., 2006; Newcomb et al., 2006]. One hypothesis for changes in cell number is that cell number might be correlated with the size of the target organ [Marois and Carew, 1997; Page and Parries, 2000]. Because the Pd5 and Pd6 cells in *T. diomedea* are motor neurons involved in crawling, we hypothesized that the number of large, TPep-LIR cells in the pedal ganglia would be correlated with the size of the foot. Additionally, within an individual species, cell size appears to be correlated with the innervation area [Gillette, 1991; Moroz et al., 1997]. Motor neurons with large target areas tend to have large somas, whereas interneurons and sensory neurons, which tend to have smaller target areas, have smaller somas [Gillette, 1991]. Because cell size is correlated with innervation area within a species, we hypothesized that target area should also be correlated with the size of motor neurons across species.

Using immunohistochemistry, we found that the presence of large, TPep-LIR cells similar to the Pd5 and Pd6 cells in *T. diomedea* was conserved across the nudibranchs. All species examined had 2–7 large, TPep-LIR cells in each pedal ganglion. By mapping the number of cells onto a nudibranch phylogeny, it appears that the number of cells has changed multiple times within the nudibranchs. Using independent contrasts methods, we found that the size of the largest TPep-LIR neurons was positively correlated with the size of the foot. However, the relative size of the TPep-LIR cells, calculated as the width of the cell divided by the width of the pedal ganglion, was not correlated with the foot size; therefore, the correlation between motor neuron size and foot size might be an effect of scaling rather than an effect of selection for larger cells in species with a larger foot. We also found that the number of TPep-LIR cells was not correlated with foot width. Therefore, although the presence of two or more large, TPep-LIR cells in all species of nudibranchs suggests that part of the neural circuitry controlling crawling in nudibranchs is conserved, the number of motor neurons is evolutionarily labile but is not directly related to foot size.

Materials and Methods

Animal Collection

All animals were collected within the state of Washington, USA. *Tritonia diomedea* and *Dendronotus iris* were trawled from Bellingham Bay at depths of approximately 30 m. *Tritonia festiva* and *Armina californica* were collected from Dash Point State Park and Seahurst Park by SCUBA divers. All other species were collected by net or by hand from the area around San Juan Island. All animals were maintained in flow-through seawater tanks at the University of Washington Friday Harbor Laboratories.

Immunohistochemistry

Ganglia were immunolabeled for TPep using a protocol modified from Beck et al. [2000]. The TPeps are a trio of 15-amino acid long peptides (TPep-PLS, TPep-PAR and TPep-NLS) that differ at positions 1, 8 and 12 [Lloyd et al., 1996]. We used antiserum to TPep-NLS that was provided by A.O.D. Willows. The central ganglia were removed from individuals representing 12 gastropod species (table 1). Brain samples were fixed at 4°C for 5 to 12 h in 4% paraformaldehyde in filtered sea water (FSW) with 50 mM Tris and subsequently rinsed twice in FSW, then three times in PBS (phosphate buffer, saline), at room temperature for at least 2 h. The brains were permeabilized in PTA (PBS with 4% Triton-X 100 and 0.1% NaN_3) for 12 to 24 h, then incubated at 4°C in PTA with 6% normal donkey serum (NDS) for 6–12 h, followed by incubation at 4°C in PTA, 6% NDS, and 0.2% rabbit anti-TPep-NLS [Willows et al., 1997] for 24–48 h. After being rinsed 5 times in PTA over 12 h at room temperature, the central ganglia were incubated at 4°C in PTA with 6% NDS for 12–24 h, then incubated at 4°C in PTA, 6% NDS, and 0.125% Alexafluor 488 donkey anti-rabbit IgG (Molecular Probes, Eugene, Oregon, USA) for 24–48 h. Brains were then rinsed at room temperature 5 times in PBS over 12 h. Finally, the brains were dehydrated through an ethanol series, cleared with xylenes, and mounted in DPX.

As a control, the secondary antibody was omitted from the second incubation solution. None of the control tissue showed any TPep-like immunolabeling. To control for non-specific labeling by the secondary antibody, brains were incubated without the TPep-NLS antiserum. Again, none of this control tissue showed labeling by the secondary antibody. To control for non-specific

Table 1. Summary of species examined for TPep-like immunoreactivity in the central ganglia

Subclass Opisthobranchia	
Order Nudibranchia	
Suborder Aeolidoidea	*Aeolidia papillosa*
	Hermissenda crassicornis
Suborder Arminoidea	*Armina californica*
	Dirona albolineata
	Janolus fuscus
Suborder Dendronotoidea	*Dendronotus albus*
	Dendronotus iris
	Melibe leonina
	Tritonia diomedea
	Tritonia festiva
Suborder Doridoidea	*Cadlina leutomarginata*
	Rostanga pulchra

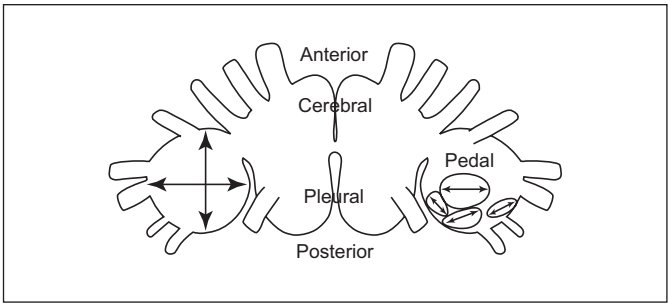

Fig. 1. Schematic diagram of the central ganglia of *Tritonia diomedea*. Brain is shown dorsal-side up. The width of the ganglion was measured at the widest point along the anterior-posterior axis and at the widest point along the transverse axis. The width of the TPep-like immunoreactive (TPep-LIR) neurons was measured along the longest visible axis.

labeling of our primary antibody, we added 100 μM TPep-NLS to our primary antibody solution 24 h before incubating the tissue in the antibody solution. We processed brains from *Armina californica* with the pre-incubated primary antibody. Tissue that was processed with the pre-incubated TPep-NLS antiserum did not show any TPep-like immunolabeling. All TPep-immunolabeling was imaged with a Bio-Rad Radiance confocal microscope and captured using Bio-Rad LaserSharp2000 software (Bio-Rad Laboratories, Hercules, Calif., USA).

One of the *T. diomedea* brains used for statistical analyses was previously immunolabeled with a TPep-NLS antibody by Shaun D. Cain using a similar protocol [unpublished data]. The *T. diomedea* brain immunolabeled with a TPep-NLS antibody published in Beck et al. [2000] was also used for statistical analyses.

Size Measurements

Measurements of cell size and ganglion width were made in NIH ImageJ 1.32. To control for variation in animal size among species, we standardized cell size by dividing cell width by ganglion width. This ratio is termed 'relative cell size'. The width of the TPep-LIR cells was measured along the longest visible axis (fig. 1). The width of the ganglion was measured at the widest point along the anterior-posterior axis and at the widest point along the transverse axis. For most species, when viewing the dorsal surface, the pedal ganglia were roughly circular. However, for some species, such as *D. albolineata*, the ganglia tended to be wider along the transverse axis than they were along the anterior-posterior axis. Other species, such as *D. iris* tended to be wider along the anterior-posterior axis. Therefore, for each individual, we used the longer axis for our measurement of ganglion width.

Neurons were designated as 'large' if the relative cell size was greater than 0.10, meaning the cell width was greater than 10% of the width of the pedal ganglion. This value was chosen on the basis of measurements of the *T. diomedea* TPep-LIR cells in Beck et al. [2000]. On the dorsal surface of each pedal ganglion in this species, there were three prominent cells (Pd5, Pd6 and Pedal 7 (Pd7)) that all exceeded a relative cell size of 0.20. A fourth cell was slightly smaller and had a relative size of 0.11 on the left pedal ganglion and 0.16 on the right pedal ganglion. The next biggest cell appeared distinctly smaller and had a relative size of 0.07 on the left pedal ganglion and 0.09 on the right pedal ganglion. Therefore, a relative cell size of 0.10 was selected as the cut-off between 'medium' and 'large' cells.

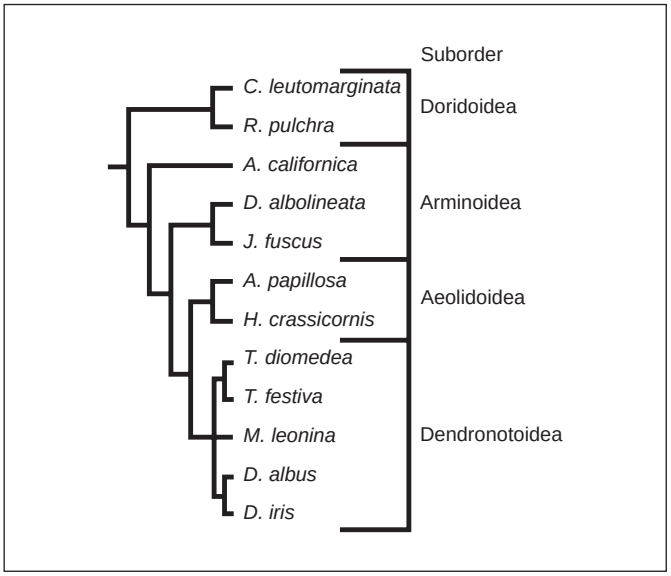

Fig. 2. Nudibranch phylogeny used for independent contrasts analyses. The relationship between suborders is a summary of phylogenies based on morphological characteristics and molecular markers [Wägele and Willan, 2000; Wollscheid-Lengeling et al., 2001]. *Tritonia diomedea* and *Tritonia festiva* are grouped together based on their taxonomic classification, as are *Dendronotus iris* and *Dendronotus albus*.

Measurements of foot size were made in Adobe Illustrator from images of adults of each species while the animals were crawling. We measured the length of foot along the midline. We

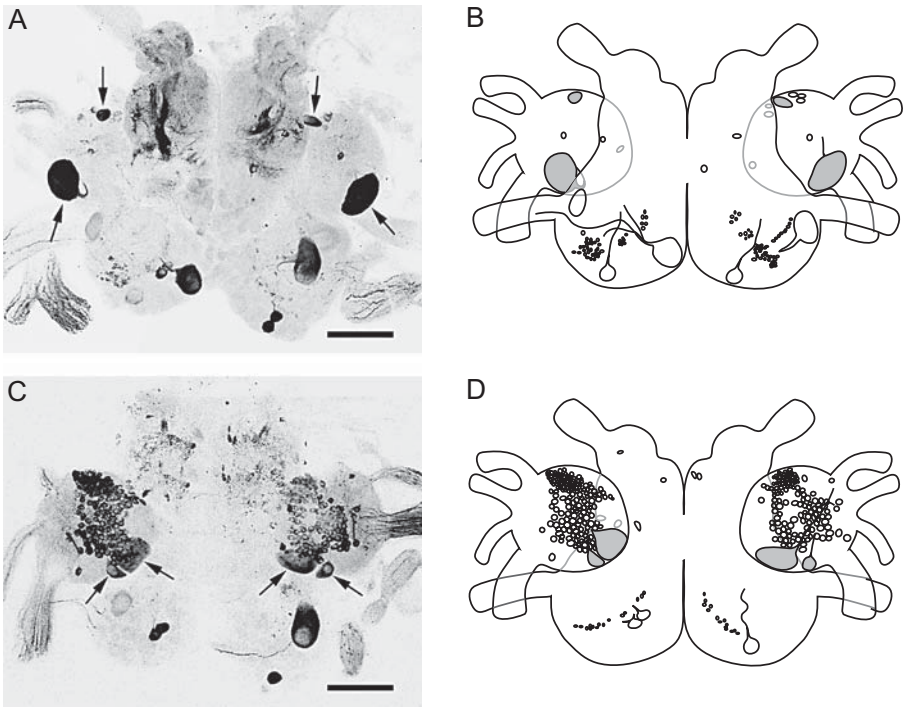

Fig. 3. TPep-like immunolabeling in *Cadlina leutomarginata*. **A** TPep-like immunoreactivity on the dorsal surface of the central ganglia of *C. leutomarginata*. Arrows indicate the large TPep-LIR neurons in the pedal ganglia. Brightness and contrast were adjusted in Adobe Photoshop. Scale bar = 250 μm. **B** Schematic diagram summarizing TPep-LIR neurons on the dorsal surface of the central ganglia. The large TPep-LIR cells are shaded. The ganglia, nerves and cell bodies were traced from confocal micrographs in Adobe Illustrator. The projection patterns of neurites were determined using NIH ImageJ. **C** TPep-like immunoreactivity on the ventral surface of the central ganglia. Arrows indicate the large TPep-LIR neurons in the pedal ganglia. Scale bar = 250 μm. **D** Schematic diagram summarizing TPep-LIR neurons on the ventral surface of the central ganglia. The large TPep-LIR cells are shaded.

measured the width of the foot perpendicular to the midline halfway along the length of the foot. The shape of the foot varies greatly depending on the behavioral state of the animal, but while crawling the foot is flat and maintains a relatively constant shape [Copeland, 1919, 1922; Audesirk, 1978]. Because foot length and width are correlated, we performed a principal component analysis in MATLAB (The Mathworks, Natick, MA) to collapse length and width into the single variable 'foot size'.

Data Analysis

When making comparisons among phenotypic traits in multiple species, data points are not statistically independent because of the hierarchal nature of phylogenetic relationships [Felsenstein, 1985; Harvey and Pagel, 1991]. Independent comparison methods use actual trait values and phylogenetic relationships to assign ancestral trait values to the nodes of the phylogeny. The assigned nodal values are then used to compare each pair of species, or pair of nodes, that share a common ancestor [Felsenstein, 1985; Harvey and Pagel, 1991]. Independent contrasts regression analyses were performed using the PDAP module in Mesquite version 1.06 [Garland et al., 1992, 1993; Midford et al., 2003; Maddison and Maddison, 2005]. The nudibranch phylogeny shown in figure 2 was used for these analyses.

To determine if the size or number of TPep-LIR cells is correlated with size, we performed independent contrasts regression analyses for: (a) the absolute size of the largest TPep-LIR cell; (b) the relative size of the largest TPep-LIR cell; and (c) the number of large TPep-LIR cells vs. the first principal component of foot length and width (i.e., foot size). The number of cells used in the analyses was the number of individually identifiable TPep-LIR cells with a relative cell size greater than 0.10.

The results of independent contrasts regression analyses are affected by the branch lengths assigned to the phylogeny. There are various methods available in Mesquite for assigning branch lengths. One of the assumptions of independent contrasts regression analyses is that there is no correlation between the size of the contrast value and its standard deviation [Pagel, 1992]. To determine which method we should use to assign branch lengths, we examined the relationship between the size of the contrast value and its standard deviation for each variable when branch lengths were assigned using a number of methods available in Mesquite. There was no method of assigning branch length available that produced no significant correlations for all the variables tested. By assigning 'All Branch Lengths to 1.0' then 'Branch Length Method of Nee', followed by 'Grafen's [1989] Rho transform' with Rho = 0.5, there were no significant correlations between the size of the contrast value and its standard deviation for any of the variables tested. This method was therefore used to assign branch lengths for independent contrasts regression analyses.

Results

Immunohistochemistry

Suborder Doridoidea

Cadlina leutomarginata. In *C. leutomarginata*, both the right and left pedal ganglia had four large, TPep-LIR cells (fig. 3). Two cells were located on the dorsal surface

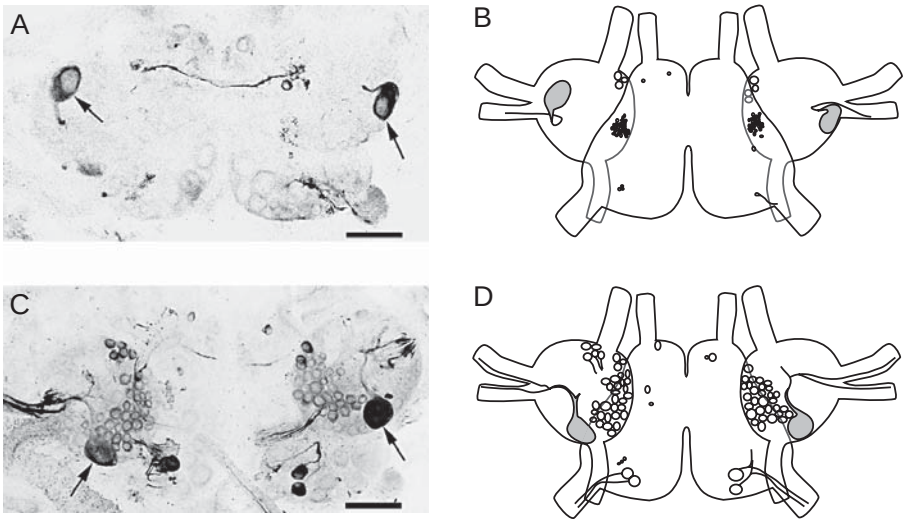

Fig. 4. TPep-like immunolabeling in *Rostanga pulchra*. **A** TPep-like immunoreactivity on the dorsal surface of the central ganglia of *R. pulchra*. Arrows indicate the large TPep-LIR neurons in the pedal ganglia. Brightness and contrast were adjusted in Adobe Photoshop. Scale bar = 125 μm. **B** Schematic diagram summarizing TPep-LIR neurons on the dorsal surface of the central ganglia. The large TPep-LIR cells are shaded. **C** TPep-like immunoreactivity on the ventral surface of the central ganglia. Arrows indicate the large TPep-LIR neurons in the pedal ganglia. Scale bar = 125 μm. **D** Schematic diagram summarizing TPep-LIR neurons on the ventral surface of the central ganglia. The large TPep-LIR cells are shaded.

Table 2. Summary of foot dimensions and of large TPep-LIR cells in the pedal ganglia

Species	Cells	Largest right pedal cell			Largest left pedal cell			Foot dimensions		
		n	cell width (μm ± SE)	relative size (± SE)	n	cell width (μm ± SE)	relative size (± SE)	n	length (mm ± SE)	width (mm ± SE)
C. leutomarginata	4	4	186 ± 7	0.36 ± 0.03	4	173 ± 8	0.34 ± 0.02	2	29 ± 6	9 ± 2
R. pulchra	2	3	92 ± 1	0.27 ± 0.01	3	97 ± 3	0.29 ± 0.02	5	19 ± 4	7 ± 1
A. californica	7	5	146 ± 21	0.18 ± 0.02	6	155 ± 13	0.19 ± 0.01	2	76 ± 8	32 ± 1
D. albolineata	5	3	195 ± 10	0.26 ± 0.03	3	183 ± 24	0.23 ± 0.01	7	46 ± 4	14 ± 1
J. fuscus	4	4	121 ± 5	0.25 ± 0.02	4	128 ± 2	0.24 ± 0.01	2	54 ± 16	16 ± 4
A. papillosa	5	3	202 ± 24	0.27 ± 0.01	3	212 ± 36	0.28 ± 0.02	2	42 ± 4	11 ± 1
H. crassicornis	3	3	129 ± 23	0.24 ± 0.02	3	133 ± 19	0.24 ± 0.01	3	30 ± 3	7 ± 2
T. diomedea	4	3	287 ± 22	0.28 ± 0.05	3	296 ± 37	0.30 ± 0.04	3	171 ± 15	71 ± 4
T. festiva	4	3	232 ± 8	0.31 ± 0.01	3	221 ± 35	0.31 ± 0.05	2	67 ± 16	24 ± 7
M. leonina	2	7	134 ± 20	0.19 ± 0.01	6	127 ± 16	0.18 ± 0.01	5	66 ± 8	8 ± 1
D. albus	3	4	203 ± 12	0.43 ± 0.03	4	185 ± 9	0.37 ± 0.03			
D. iris	3	3	276 ± 43	0.12 ± 0.01	3	273 ± 24	0.13 ± 0.01			

and two were on the ventral surface. The largest cell, located on the dorsal surface, had a mean width of 186 ± 7 μm (mean ± SE; n = 4) in the right pedal ganglion and 173 ± 8 μm (n = 4) in the left pedal ganglion (table 2). In the right pedal ganglion, the mean relative cell size (cell width divided by ganglion width) of the largest TPep-LIR cell was 0.36 ± 0.03. In the left pedal ganglion, the mean relative cell size was 0.34 ± 0.02.

Rostanga pulchra. *R. pulchra* had two large, TPep-LIR cells in each pedal ganglion (fig. 4). The largest cell, located on the ventral surface, had a mean width of 92 ± 1 μm (n = 3) in the right pedal ganglion and 97 ± 3 μm (n = 3) in the left pedal ganglion, with a mean relative size of 0.27 ± 0.01 in the right pedal ganglion and 0.29 ± 0.02 in the left pedal ganglion. The large TPep-LIR cell on the ventral surface in each ganglion had three major branches. One branch projected towards the anterior nerve of the pedal ganglion, one branch entered the anterolateral nerve of the pedal ganglion, and one entered the posterolateral nerve. The large TPep-LIR cell on the dorsal surface in each ganglion had a major branch that projected out the posterolateral nerve.

There was a cluster of 30–35 TPep-LIR cells on the medial margin of the ventral surface of each pedal ganglion. In one specimen, the largest one of these cells had a relative size of 0.11 in the right pedal ganglion and 0.10

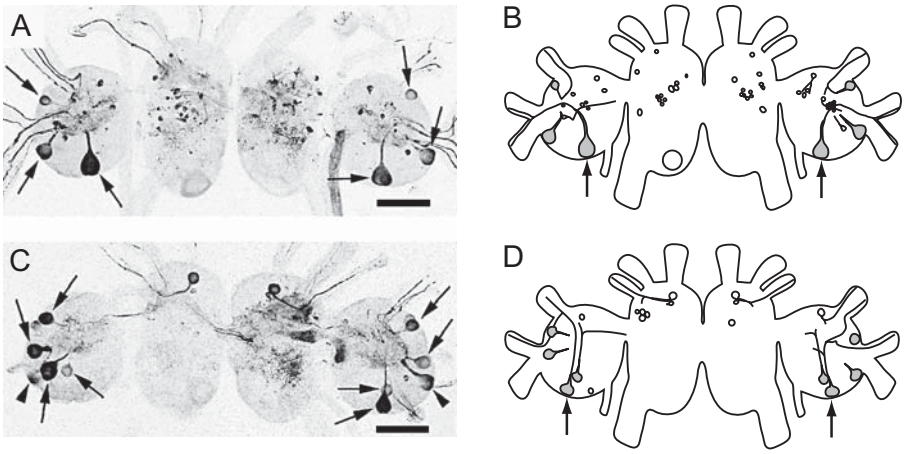

Fig. 5. TPep-like immunolabeling in *Armina californica*. **A** TPep-like immunoreactivity on the dorsal surface of the central ganglia of *A. californica*. Arrows indicate the large TPep-LIR neurons in the pedal ganglia. Brightness and contrast were adjusted in Adobe Photoshop. Scale bar = 250 μm. **B** Schematic diagram summarizing TPep-LIR neurons on the dorsal surface of the central ganglia. The large TPep-LIR cells are shaded. Arrows indicate likely homologues of the Pd5 neurons in *T. diomedea*. **C** TPep-like immunoreactivity on the ventral surface of the central ganglia. Arrows indicate the large TPep-LIR neurons in the pedal ganglia. The cells indicated by arrowheads are the same cells as the large TPep-LIR cells located at the posterolateral margin of the dorsal surface. Scale bar = 250 μm. **D** Schematic diagram summarizing TPep-LIR neurons on the ventral surface of the central ganglia. The large TPep-LIR cells are shaded. Arrows indicate likely homologues of the Pd6 neurons in *T. diomedea*.

in the left pedal ganglion. This cell was not reliably identifiable in other specimens and is therefore not included in the regression analyses of the number of large TPep-LIR cells vs. foot length, width and area (table 2).

Suborder Arminoidea

Armina californica. The right pedal ganglia of five animals were immunolabeled. The largest TPep-LIR cell was located near the posterior edge of the dorsal surface of the ganglion (fig. 5). This cell had a mean width of 146 ± 21 μm and a mean relative size of 0.18 ± 0.02. There were six additional large, TPep-LIR cells, with mean relative sizes ranging from 0.16 ± 0.01 to 0.11 ± 0.01.

The left pedal ganglia of six animals were immunolabeled. As in the right pedal ganglion, there was a large TPep-LIR cell near the posterior edge of the dorsal surface. This cell had a mean width of 155 ± 13 μm and a mean relative size of 0.19 ± 0.01. There were six additional large, TPep-LIR cells, with mean relative sizes ranging from 0.15 ± 0.01 to 0.10 ± 0.01.

In one of the preparations, it was possible to determine the projection pattern of some of the large, TPep-LIR cells. The largest TPep-LIR cell in both pedal ganglia had a primary neurite that bifurcated and sent a branch into each of the two lateral nerves of the pedal ganglion. The morphology of this cell is similar to that of Pd5 in *T. diomedea* and is likely a Pd5-homologue. The cell located on the posterolateral margin of the dorsal surface had a primary neurite that bifurcated and sent one branch towards the fused cerebral-pleural ganglia. The target of the second branch could not be determined. The smallest and most anterior of the large, TPep-LIR cells on the dorsal surface also appeared to have a primary neurite that bifurcated, with one branch extending into the neuropil of the pedal ganglion and a second branch projecting into the anterior nerve of the pedal ganglion.

The largest TPep-LIR cell on the ventral surface in both pedal ganglia had a primary neurite that bifurcated and sent one branch into the anterior nerve and the other branch into the anterolateral nerve. This cell is likely the homologue of the Pd6 cell in *T. diomedea*. One of the other cells on the ventral surface had a primary neurite that bifurcated and sent one branch toward the cerebral-pleural ganglia and one towards the anterior nerve of the pedal ganglion.

Dirona albolineata. All three individuals had 5 large TPep-LIR cells on the dorsal surface of the right pedal ganglion (fig. 6). The largest of these cells had a mean width of 195 ± 10 μm and a mean relative size of 0.26 ± 0.03. All 3 individuals had 5 large TPep-LIR cells on the dorsal surface of the left pedal ganglion. The largest of these cells had a mean width of 183 ± 24 μm and a mean

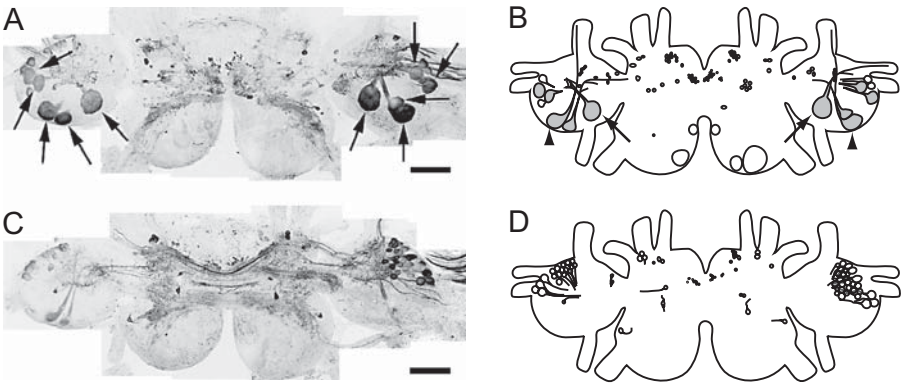

Fig. 6. TPep-like immunolabeling in *Dirona albolineata*. **A** TPep-like immunoreactivity on the dorsal surface of the central ganglia of *D. albolineata*. Arrows indicate the large TPep-LIR neurons in the pedal ganglia. Brightness and contrast were adjusted in Adobe Photoshop. Scale bar = 250 μm. **B** Schematic diagram summarizing TPep-LIR neurons on the dorsal surface of the central ganglia. The large TPep-LIR cells are shaded. Arrows indicate likely homologues of the Pd5 neurons in *T. diomedea*. Arrowheads indicate likely homologues of the Pd6 neurons in *T. diomedea*. **C** TPep-like immunoreactivity on the ventral surface of the central ganglia. Scale bar = 250 μm. **D** Schematic diagram summarizing TPep-LIR neurons on the ventral surface of the central ganglia.

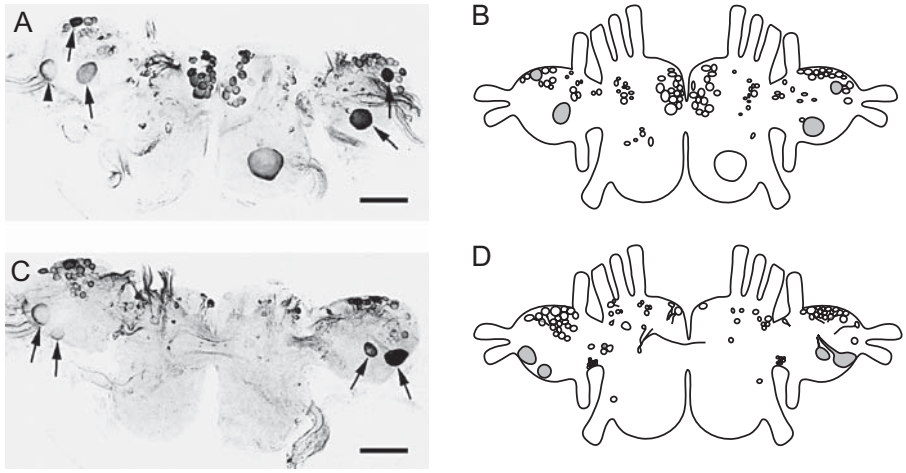

Fig. 7. TPep-like immunolabeling in *Janolus fuscus*. **A** TPep-like immunoreactivity on the dorsal surface of the central ganglia of *J. fuscus*. Arrows indicate the large TPep-LIR neurons in the pedal ganglia. The cell indicated by arrowhead is the same cell as the large TPep-LIR cell located at the lateral margin of the ventral surface. Brightness and contrast were adjusted in Adobe Photoshop. Scale bar = 250 μm. **B** Schematic diagram summarizing TPep-LIR neurons on the dorsal surface of the central ganglia. The large TPep-LIR cells are shaded. **C** TPep-like immunoreactivity on the ventral surface of the central ganglia. Arrows indicate the large TPep-LIR neurons in the pedal ganglia. Scale bar = 250 μm. **D** Schematic diagram summarizing TPep-LIR neurons on the ventral surface of the central ganglia. The large TPep-LIR cells are shaded.

relative size of 0.23 ± 0.01. There was also a cluster of five or six TPep-LIR cells on the lateral margin of both pedal ganglia. In one specimen, two of these cells in the left pedal ganglion had a relative size greater than 0.10 (actual value = 0.11 and 0.12). In another specimen, one of these cells in the right pedal ganglion had a relative size greater than 0.10 (actual value = 0.12) and one of these cells in the left pedal ganglion had a relative size greater than 0.10 (actual value = 0.11). However, because these cells were not individually identifiable in other specimens, they were not included in the regression analysis of the number of large TPep-LIR cells vs. foot size.

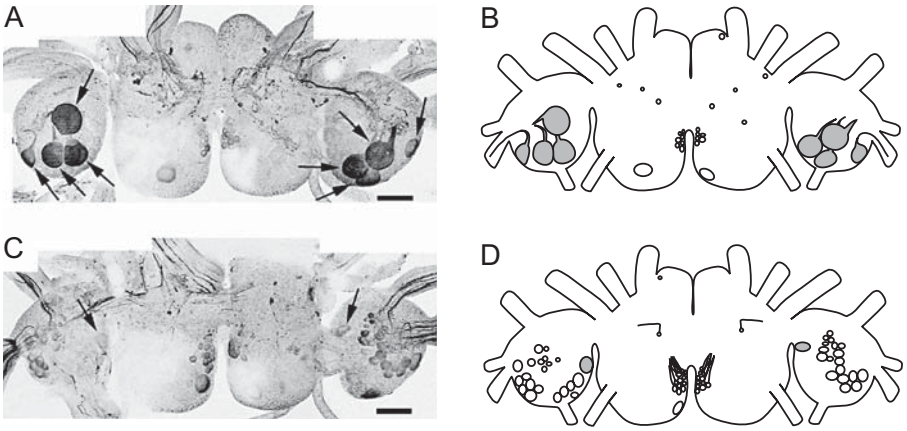

Fig. 8. TPep-like immunolabeling in *Aeolidia papillosa*. **A** TPep-like immunoreactivity on the dorsal surface of the central ganglia of *A. papillosa*. Arrows indicate the large TPep-LIR neurons in the pedal ganglia. Brightness and contrast were adjusted in Adobe Photoshop. Scale bar = 250 μm. **B** Schematic diagram summarizing TPep-LIR neurons on the dorsal surface of the central ganglia. The large TPep-LIR cells are shaded. **C** TPep-like immunoreactivity on the ventral surface of the central ganglia. Arrows indicate the large TPep-LIR neurons in the pedal ganglia. Scale bar = 250 μm. **D** Schematic diagram summarizing TPep-LIR neurons on the ventral surface of the central ganglia. The large TPep-LIR cells are shaded.

In both ganglia, the primary neurite of the largest and most medial TPep-LIR cell bifurcated. It appeared to send one branch out the anterolateral nerve of the pedal ganglion and the second branch towards the posterolateral nerve. Based on morphology, this cell is likely homologous to the *T. diomedea* Pd5 cell. The second largest cell, located on the posterior margin of the pedal ganglion, also had a primary neurite that bifurcated, sending one branch into the anterior nerve of the pedal ganglion and sending the other branch towards the lateral nerves. This cell is likely homologous to the *T. diomedea* Pd6 cell. One of the other large, TPep-LIR cells appeared to send a neurite into the ipsilateral cerebral-pleural ganglion.

Janolus fuscus. Four animals were examined. There were 4 large TPep-LIR cells in each pedal ganglion. The largest TPep-LIR cell in the right pedal ganglion had a mean width of 121 ± 5 μm and a mean relative size of 0.25 ± 0.02 (fig. 7). The largest TPep-LIR cell in the left pedal ganglion had a mean width of 128 ± 2 μm and a mean relative size of 0.24 ± 0.01.

Suborder Aeolidoidea

Aeolidia papillosa. *A. papillosa* had 4 large, TPep-LIR cells on the dorsal surface of the right pedal ganglion (fig. 8). The largest of the cells was had a mean width of 202 ± 24 μm and a mean relative size of 0.27 ± 0.01 (n = 3). Likewise, there were 4 large, TPep-LIR neurons on the dorsal surface of the left pedal ganglion. The largest of the cells had a mean width of 212 ± 36 μm and a mean relative size of 0.28 ± 0.02 (n = 3). There was also one large TPep-LIR cell on the medial margin of each pedal ganglion. The smallest and most lateral of the large, TPep-LIR cells appeared to have a primary neurite that projected into the posterolateral nerve of the pedal ganglion.

Hermissenda crassicornis. *H. crassicornis* had 3 large, TPep-LIR cells on the dorsal surface of the right pedal ganglion (fig. 9). The largest of the cells had a mean width of 129 ± 23 μm and a mean relative size of 0.24 ± 0.02 (n = 3). There were also 3 large TPep-LIR cells on the dorsal surface of the left pedal ganglion. The largest of the cells had a mean width of 133 ± 19 μm and a mean relative size of 0.24 ± 0.01 (n = 3). There was also a cluster of about 15 TPep-LIR cells on the lateral margin of both pedal ganglia. In one specimen, one of these cells in the right pedal ganglion had a relative size greater than 0.10 (actual value = 0.10) and one of these cells in the left pedal ganglion had a relative size greater than 0.10 (actual value = 0.13). In another specimen, one of these cells in the left pedal ganglion had a relative size greater than 0.10 (actual value = 0.10). However, because these cells were not individually identifiable in other specimens, they were not included in the regression analyses of the number of large TPep-LIR cells vs. foot length, width and area.

The largest TPep-LIR cell in each pedal ganglion appeared to send a neurite into the lateral nerve of the pedal ganglion. Based on its morphology, this cell is likely

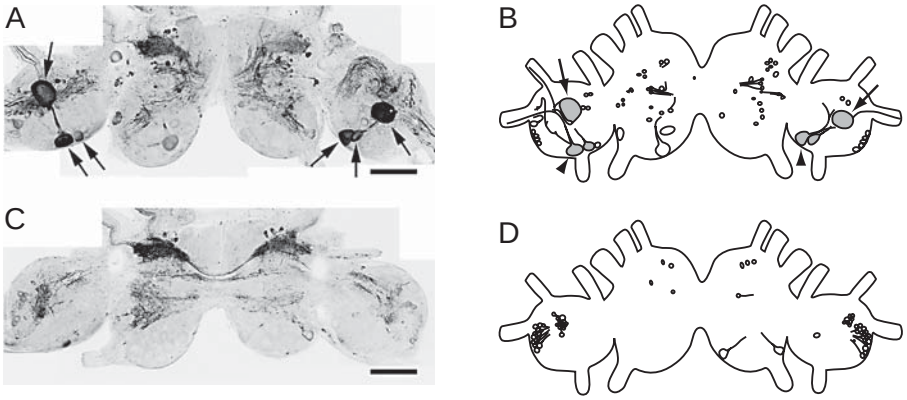

Fig. 9. TPep-like immunolabeling in *Hermissenda crassicornis*. **A** TPep-like immunoreactivity on the dorsal surface of the central ganglia of *H. crassicornis*. Arrows indicate the large TPep-LIR neurons in the pedal ganglia. Brightness and contrast were adjusted in Adobe Photoshop. Scale bar = 250 μm. **B** Schematic diagram summarizing TPep-LIR neurons on the dorsal surface of the central ganglia. The large TPep-LIR cells are shaded. Arrows indicate likely homologues of the *T. diomedea* Pd5 neurons. Arrowheads indicate likely homologues of the Pd6 neurons in *T. diomedea*. **C** TPep-like immunoreactivity on the ventral surface of the central ganglia. Scale bar = 250 μm. **D** Schematic diagram summarizing TPep-LIR neurons on the ventral surface of the central ganglia.

homologous to the Pd5 cell in *T. diomedea*. The primary neurite of the second largest TPep-LIR cell had three branches. One branch of the neurite projected into the lateral nerve of the pedal ganglion. A second branch projected into the anterior nerve of the pedal ganglion. The third branch projected into the neuropil of the pedal ganglion. This cell might be homologous to the *T. diomedea* Pd6 neuron.

Suborder Dendronotoidea

Tritonia diomedea. All specimens had 4 large, TPep-LIR cells on the dorsal surface of both the right and left pedal ganglion (n = 3). The largest cell had a mean width of 287 ± 22 μm (mean relative size: 0.28 ± 0.05) in the right pedal ganglion and a mean width of 296 ± 37 μm (mean relative size: 0.30 ± 0.04) in the left pedal ganglion.

There was a group of 8–10 TPep-LIR cells on the ventral surface of each pedal ganglion. In each specimen, at least 2 of these cells in the right pedal ganglion and 3 of these cells in the left pedal ganglion had a relative size greater than 0.10. However, we could not be sure that we were measuring the same cells in each specimen. Therefore, these cells were not included in the regression analyses.

Tritonia festiva. *T. festiva* had 4 large, TPep-LIR cells on the dorsal surface of each pedal ganglion (fig. 10). The biggest cell had a mean width of 232 ± 8 μm (mean relative size: 0.31 ± 0.01; n = 3) in the right pedal ganglion and a mean width of 221 ± 35 μm (mean relative size: 0.31 ± 0.05; n = 3) in the left pedal ganglion.

There was a group of 8–10 TPep-LIR cells on the ventral surface of each pedal ganglion. In each specimen, at least 1 of these cells in the right pedal ganglion and 2 of these cells in the left pedal ganglion had a relative size greater than 0.10. However, we could not be sure that we were measuring the same cells in each specimen. Therefore, these cells were not included in the regression analyses.

Melibe leonina. The right pedal ganglia from 7 animals and the left pedal ganglia from 6 animals were immunolabeled. All specimens had one large TPep-LIR cell on the dorsal surface of each pedal ganglion and one large TPep-LIR cell on the ventral surface (fig. 11). The cell on the ventral surface was the larger of the two cells. This cell had a mean width of 134 ± 20 μm (mean relative size: 0.19 ± 0.01) in the right pedal ganglion and a mean width of 127 ± 16 μm (mean relative size: 0.18 ± 0.01) in the left pedal ganglion.

The primary neurite from the large TPep-LIR cell on the dorsal surface projected toward the lateral nerves of the pedal ganglion. This cell is likely homologous to the *T. diomedea* Pd5 cell. The primary neurite from the large TPep-LIR cell on the ventral surface of the right pedal ganglion branched several times in the neuropil. One branch projected out the anterior nerve of the pedal ganglion. This neuron might be a homologue of the Pd6 cell in *T. diomedea*.

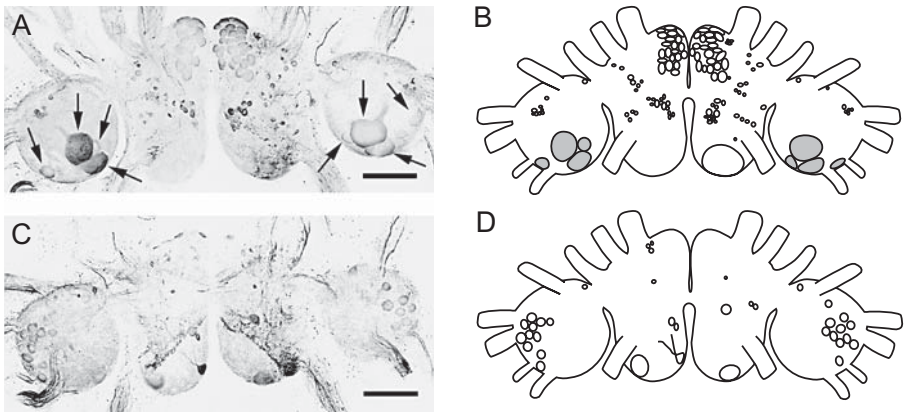

Fig. 10. TPep-like immunolabeling in *Tritonia festiva*. **A** TPep-like immunoreactivity on the dorsal surface of the central ganglia of *T. festiva*. Arrows indicate the large TPep-LIR neurons in the pedal ganglia. Brightness and contrast were adjusted in Adobe Photoshop. Scale bar = 250 μm. **B** Schematic diagram summarizing TPep-LIR neurons on the dorsal surface of the central ganglia. The large TPep-LIR cells are shaded. **C** TPep-like immunoreactivity on the ventral surface of the central ganglia. Scale bar = 250 μm. **D** Schematic diagram summarizing TPep-LIR neurons on the ventral surface of the central ganglia.

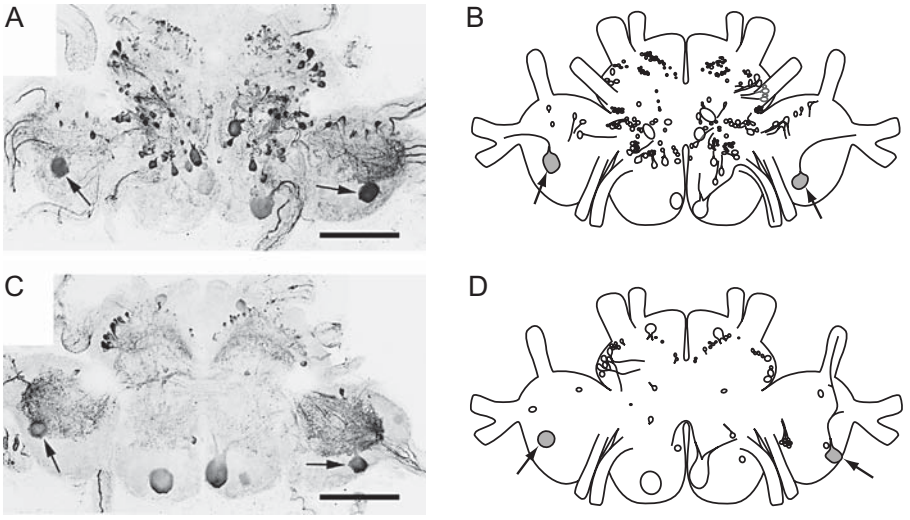

Fig. 11. TPep-like immunolabeling in *Melibe leonina*. **A** TPep-like immunoreactivity on the dorsal surface of the central ganglia of *M. leonina*. Arrows indicate the large TPep-LIR neurons in the pedal ganglia. Brightness and contrast were adjusted in Adobe Photoshop. Scale bar = 250 μm. **B** Schematic diagram summarizing TPep-LIR neurons on the dorsal surface of the central ganglia. The large TPep-LIR cells are shaded. Arrows indicate likely homologues of the Pd5 neurons in *T. diomedea*. **C** TPep-like immunoreactivity on the ventral surface of the central ganglia. Arrows indicate the large TPep-LIR neurons in the pedal ganglia. Scale bar = 250 μm. **D** Schematic diagram summarizing TPep-LIR neurons on the ventral surface of the central ganglia. The large TPep-LIR cells are shaded. Arrows indicate likely homologues of the Pd6 neurons in *T. diomedea*.

Dendronotus albus. *D. albus* had 1 large, TPep-LIR cell on the dorsal surface of each pedal ganglion (fig. 12). There were 2 large TPep-LIR cells on the ventral surface of each pedal ganglion. The largest cell had a mean width of 203 ± 12 μm (mean relative size: 0.43 ± 0.03; n = 4) in the right ganglion and a mean width of 185 ± 9 μm (mean relative size: 0.37 ± 0.03; n = 4) in the left ganglion.

There was also a group of about 20 TPep-LIR cells on the ventral surface of each pedal ganglion. In each specimen, 10–12 of these cells have a relative size between 0.15 and 0.20. However, this cluster appeared more sim-

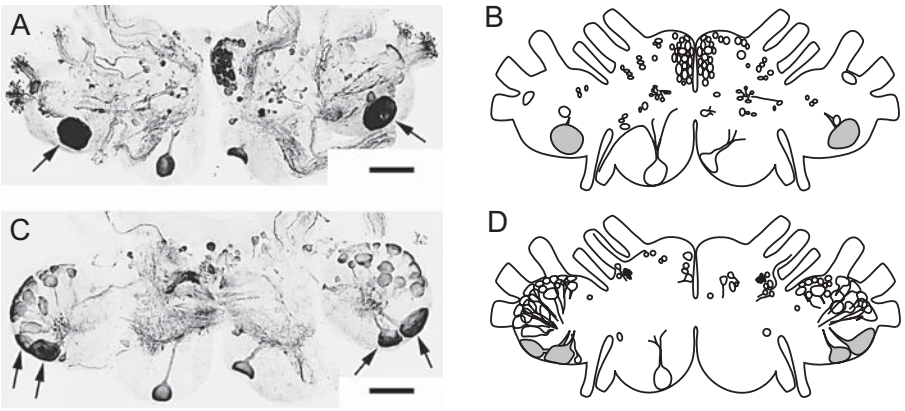

Fig. 12. TPep-like immunolabeling in *Dendronotus albus*. **A** TPep-like immunoreactivity on the dorsal surface of the central ganglia of *D. albus*. Arrows indicate the large TPep-LIR neurons in the pedal ganglia. Brightness and contrast were adjusted in Adobe Photoshop. Scale bar = 250 μm. **B** Schematic diagram summarizing TPep-LIR neurons on the dorsal surface of the central ganglia. The large TPep-LIR cells are shaded. **C** TPep-like immunoreactivity on the ventral surface of the central ganglia. Arrows indicate the large TPep-LIR neurons in the pedal ganglia. Scale bar = 250 μm. **D** Schematic diagram summarizing TPep-LIR neurons on the ventral surface of the central ganglia. The large TPep-LIR cells are shaded.

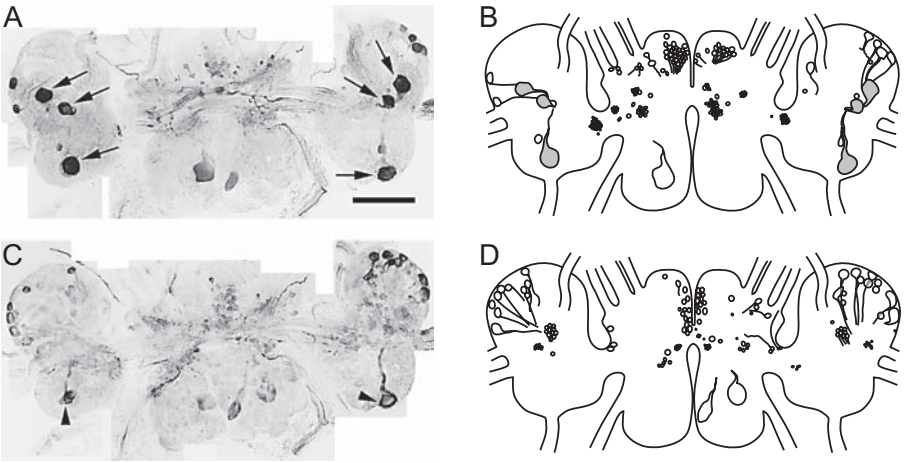

Fig. 13. TPep-like immunolabeling in *Dendronotus iris*. **A** TPep-like immunoreactivity on the dorsal surface of the central ganglia of *D. iris*. Arrows indicate the large TPep-LIR neurons in the pedal ganglia. Brightness and contrast were adjusted in Adobe Photoshop. Scale bar = 1000 μm. **B** Schematic diagram summarizing TPep-LIR neurons on the dorsal surface of the central ganglia. The large TPep-LIR cells are shaded. **C** TPep-like immunoreactivity on the ventral surface of the central ganglia. The cells indicated by arrowheads are the same cells as the large TPep-LIR cells located at the posterior margin of the dorsal surface. Scale bar = 1000 μm. **D** Schematic diagram summarizing TPep-LIR neurons on the ventral surface of the central ganglia.

ilar to a cluster of smaller TPep-LIR cells on the ventral surface of the pedal ganglia found in *D. iris*, *T. diomedea* and *T. festiva* rather than to the Pd5 and Pd6 cells. Therefore, we did not include these cells in our regression analyses of cell number vs. foot length, foot width and foot area.

Dendronotus iris. *D. iris* had 3 large, TPep-LIR cells on the dorsal surface of the each pedal ganglion (fig. 13). The largest cell had a mean width of 276 ± 43 μm (mean relative size: 0.12 ± 0.01; n = 3) in the right ganglion and a mean width of 273 ± 24 μm (mean relative size: 0.13 ± 0.01; n = 3) in the left ganglion.

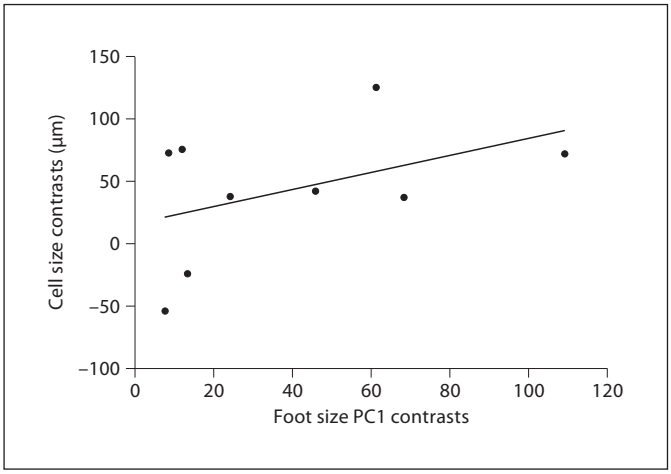

Fig. 14. Independent contrasts regression of cell size against foot size. Foot size was determined by performing a principal components analysis of foot length and foot width. Independent contrast values for foot size and cell size were generated in the PDAP module in Mesquite version 1.06 [Midford et al., 2003; Maddison and Maddison, 2005]. Independent comparison methods use actual trait values and phylogenetic relationships to assign ancestral trait values to the nodes of the phylogeny. The assigned nodal values are then used to compare each pair of species, or pair of nodes, that share a common ancestor. As a result, a data set with 10 species will generate 9 nodal values used for the regression analysis.

Foot Size Measurements

Foot size measurements were not made on the animals collected for immunohistochemistry, but we were able to collect at least 2 additional specimens from 10 of the 12 species examined. The mean length and width of the foot for each species is listed in table 2. Because length and width are correlated, we performed a principal component analysis to compress the data into a single variable. The first principal component accounted for 90.3% of the total variance. We termed the transformed data 'foot size' and used this variable to perform regression analyses and ANOVAs.

Regressions and ANOVAs

To determine whether cell size was correlated with the size of the target area, we performed independent contrast regression analyses of the width of the largest TPep-LIR cell in the pedal ganglia vs. foot size. The width of the largest TPep-LIR cell was significantly correlated with foot size (right pedal ganglion: $r^2 = 0.41$, $F_{1,8} = 5.539$, $p = 0.046$; left pedal ganglion: $r^2 = 0.50$, $F_{1,8} = 8.017$, $p = 0.022$; fig. 14). However, larger animals tend to have larger pedal ganglia. Independent contrast regression analyses of pedal ganglion width vs. foot size showed a significant correlation between the variables (right pedal ganglion: $r^2 = 0.67$, $F_{1,8} = 16.286$, $p = 0.004$; left pedal ganglion: $r^2 = 0.65$, $F_{1,8} = 15.163$, $p = 0.005$). Additionally, independent contrast regression analyses of the width of the largest TPep-LIR cell vs. the width of the pedal ganglia also showed a significant correlation (right: $r^2 = 0.55$, $F_{1,10} = 11.994$, $p = 0.006$; left: $r^2 = 0.51$, $F_{1,10} = 10.222$, $p = 0.009$). Therefore, the correlation between TPep-LIR cell size and foot size might be due to larger animals having larger brains and larger brains having bigger neurons. In an effort to control for the relationship between cell size and ganglion size, we standardized cell size by dividing cell size by ganglion width to create the measurement 'relative cell size'. Independent contrasts regression analyses showed that the relative size of the largest TPep-LIR cell was not significantly correlated with the foot size (right: $r^2 < 0.001$, $F_{1,8} < 0.001$, $p = 0.986$; left: $r^2 = 0.02$, $F_{1,10} = 0.138$, $p = 0.720$).

To determine whether cell number was correlated with the size of the target area, we performed independent contrast regression analyses of the number of large TPep-LIR cell in the pedal ganglia vs. foot size. The number of large, TPep-LIR cells was the same for the right and left pedal ganglia. The number of cells was not significantly correlated with foot size ($r^2 = 0.06$, $F_{1,8} = 0.503$, $p = 0.498$).

The results of independent contrast analyses depend on the phylogeny used; however, the phylogeny of the nudibranchs is unresolved. After our initial analysis found a significant correlation between cell size and foot size, we repeated our regression analysis with the arminids *(A. californica*, *D. albolineata*, and *J. fuscus)* grouped as a monophyletic, unresolved clade, similar to the phylogeny used in Newcomb et al. [2006]. When we used this phylogeny, the correlation between cell size and foot size was still significant (right: $r^2 = 0.42$, $F_{1,8} = 5.855$, $p = 0.042$; left: $r^2 = 0.51$, $F_{1,8} = 8.315$, $p = 0.020$).

Discussion

All nudibranch species examined had at least two bilaterally symmetrical pairs of large TPep-LIR cells located on the dorsal surface of the pedal ganglia (figs. 3–13). The exact number of cells differed among species and has evidently changed multiple times in the evolutionary history of the nudibranchs (fig. 15). However, the number of large TPep-LIR cells in the pedal ganglia of a species was not correlated with foot size. This is consistent with previous studies that have shown that brain size, which is correlated with body size, is not strongly correlated with

total number of neurons in gastropods [Boyle et al., 1983; Newcomb et al., 2006].

Within an individual animal, the size of a neuron (i.e., the diameter of its soma) often reflects the size of the target area it innervates [Gillette, 1991]. A larger soma size might be an adaptation for increasing the production of cellular materials necessary to supply increases in axonal volume and innervation area [Gillette, 1991; Moroz et al., 1997]. Thus, as evolution alters the size of the foot, one possibility is that large neurons innervating specific areas of the foot might show corresponding changes in size which reflect the increased or diminished size of the target area. Our findings are consistent with this idea, inasmuch as the size of the largest TPep-LIR neuron in the pedal ganglia of a species was correlated with foot size (fig. 14). This correlation, however, must be interpreted with caution because it might also arise for reasons unrelated to the evolutionary scenario outlined above. For example, foot size is correlated with ganglion size, which in turn is correlated with cell size. In an additional analysis, we therefore standardized cell size by dividing the cell width by ganglion width. When the relative size of the largest TPep-LIR cell was compared to foot size across species, however, no significant relationship was found between relative cell size and foot size.

At least two different explanations might account for why absolute cell size is correlated with foot size but relative cell size is not. One, of course, is that the correlation between absolute cell size and target size might be due to scaling rather than to evolutionary pressures selecting for larger soma sizes in motor neurons. However, several studies have provided evidence that although there is a general trend for larger nudibranchs to have larger neurons, not all neurons increase in size as body size increases [Boyle et al., 1983; Newcomb et al., 2006]. An alternative possibility is that relative cell diameter might not be a good metric for evaluating cell size. Relative cell size was intended to control for the differences in brain size across species, but brain size is positively correlated with body size and therefore with foot size. Thus, controlling for brain size might have had the unintended consequence of controlling for foot size as well.

Implicit in the analyses of changes in cell size and cell number across species is the assumption that the large, TPep-LIR neurons in different nudibranch species are mucociliary motor neurons such as the Pd5 and Pd6 cells in *T. diomedea*. The majority of the large, TPep-LIR cells we identified have axons that project out through the pedal nerves (fig. 3–13). For example, in the arminid *A. californica*, the largest TPep-LIR cell has a primary neurite that bifurcates and sends one branch out pedal nerve 2 (PdN2) and another branch out pedal nerve 3 (PdN3) (fig. 5), a pattern matching that of the Pd5 cell in *T. diomedea* [Lohmann et al., 1991; Cain et al., 2006]. *A. californica* also has a large, TPep-LIR cell on the ventral surface of each pedal ganglion that bifurcates and sends one branch out pedal nerve 1 (PdN1) and one branch out PdN2, similar to the morphology of the *T. diomedea* Pd6 cell [Wang et al., 2003]. Additionally, the arminid *D. albolineata* (fig. 6), the aeolid *H. crassicornis* (fig. 9) and the dendronotid *M. leonina* (fig. 11) each have a large TPep-LIR cell that has branches

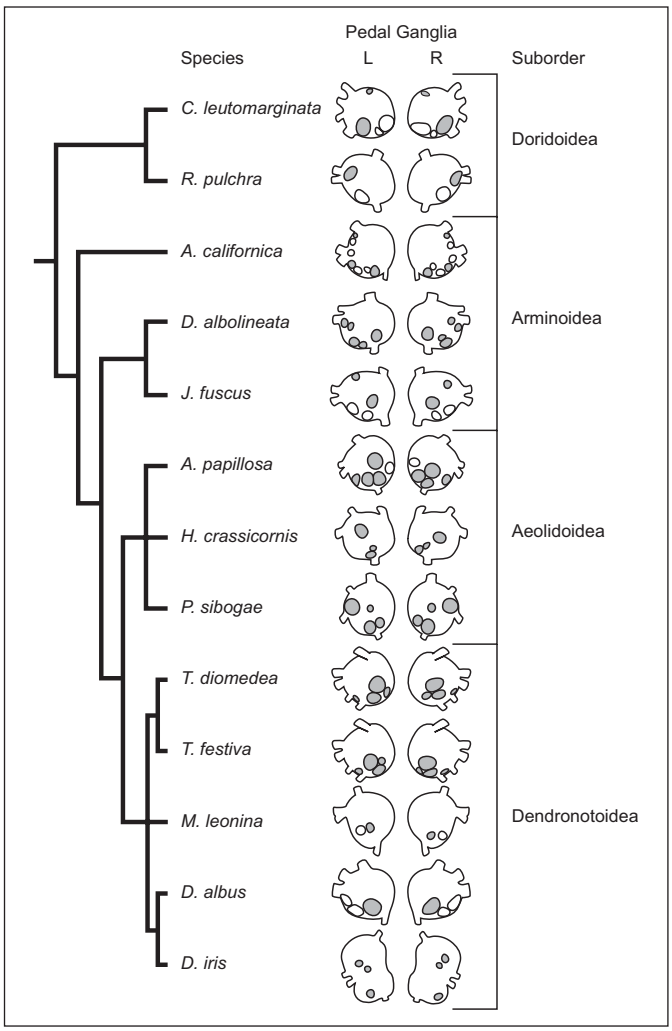

Fig. 15. Phylogeny of the nudibranchs with schematic diagrams of the large, TPep-LIR cells located in the pedal ganglia. TPep-LIR cells with a relative size greater than 0.10 are shown. The diagrams of *P. sibogae* are based on Croll et al. [2001]. Grey cells are located on the dorsal surface of the pedal ganglia. White cells are located on the ventral surface of the pedal ganglia.

projecting out PdN2 and PdN3 and a second large TPep-LIR cell that has branches projecting out PdN1 and PdN2. Axonal projection pattern, along with cell size, location, neurotransmitter content and physiology are typically used to establish homology between identifiable neurons [Weiss and Kupfermann, 1976; Nusbaum and Kristan, 1986; Croll, 1987; Watson and Willows, 1992; Breidbach and Kutsch, 1995; Wright et al., 1996; Katz et al., 2001]. The axonal projection patterns of the largest, TPep-LIR cells in the pedal ganglia of these species suggests that the largest of the TPep-LIR cells might be homologues of the Pd5 and Pd6 cells in *T. diomedea*. In the dorid *R. pulchra* (fig. 4), one of the large TPep-LIR cells projects out PdN1, PdN2 and PdN3 and another large TPep-LIR cell projects out only PdN3. Although it appears likely that one of these cells is homologous to Pd5 and the other to Pd6, it is difficult at present to determine which is which.

Using morphological and physiological features to identify homologous neurons creates two opposing sets of problems. One is that neurons, as any other structures subject to evolution, might converge on similar features without having any shared ancestry. Regardless of the criteria used to assign homology, similarities can arise from parallel evolution; thus, an element of uncertainty is inherent in any functional definition of homology [Roth, 1984]. The contrasting problem is that variation might exist in any of the morphological or physiological features used to identify evolutionarily homologous neurons [Bulloch and Ridgeway, 1995]. Indeed, these differences are often the reason why the cells are interesting from a comparative perspective. The challenge is therefore to locate neurons that share enough similarities that they can be identified as homologues, yet at the same time have enough differences that the variations can be correlated with changes in behavior or morphology.

In our study we attempted to make the identification of Pd5 and Pd6 homologues objective by choosing distinctive criteria of the Pd5 and Pd6 cells in *T. diomedea*. Among these are that the cells contain TPeps, are located on the dorsal surfaces of the pedal ganglia, and are very large (up to 500 μm in diameter). Rather than subjectively deciding what constituted a 'large' neuron in each species, we standardized cell size by dividing the width of the cell by the width of the pedal ganglion and defined a 'large' neuron as one with a soma width equal to or greater than 10% of the ganglion width. As we began imaging TPep-LIR cells in different species, however, we discovered that subjective decisions could not be avoided entirely. For example, we decided to include large TPep-LIR cells located anywhere in the pedal ganglia (not just those on the dorsal surface) because the exact location of Pd5 and Pd6 homologues might plausibly change during evolution. Similarly, we decided not to include in the analysis a cluster of about 12 TPep-LIR cells in *D. albus* (fig. 12) that fit our definition of 'large' but closely resembled a cluster of smaller TPep-LIR cells that exists in three other species: *D. iris* (fig. 13); *T. diomedea* (fig. 10); and *T. festiva* (fig. 10) (see Results for additional information).

Based on the morphological criteria typically used to identify homologous neurons, we have identified a set of potentially homologous TPep-LIR cells that are present across the nudibranchs. Although the presence of these TPep-LIR cells is conserved, the number of TPep-LIR cells varies among species. This finding is consistent with the observation that specific types of neurons tend to be conserved, but the number of cells varies among closely related species [Paul, 1991; Turrigiano and Selverston, 1991; Witten and Truman, 1998; Tierney et al., 1999; Page and Parries, 2000; Katz et al., 2001; Page, 2002; Espinoza et al., 2006; Newcomb et al., 2006]. Although the hypothesis that cell number might be correlated with the size of the target organ has been postulated several times, attempts to correlate changes in cell number with behavior or morphology have generally been unsuccessful [Faulkes and Paul, 1997; Marois and Carew, 1997; Page and Parries, 2000]. One problem in trying to correlate cell number with behavior or morphology is that the function of cells is often unknown and it is therefore difficult to know with which features cell number might be correlated. Because the Pd5 and Pd6 cells are mucociliary motor neurons, we performed regression analyses to examine the relationship between cell number and foot size and, consistent with previous studies, did not find a significant correlation. In summary, our results suggest that as motor circuits in the nudibranch nervous system evolve, both cell size and the number of motor neurons are evolutionarily labile, but cell number might not be directly related to the size of the target area.

Acknowledgements

We thank J.M. Newcomb, S.S. Burmeister and K.W. Sockman for reviewing and commenting on the work and manuscript. We thank R.C. Wyeth and O.M. Woodward for assistance collecting animals. We thank S.D. Cain and the Center for Cell Dynamics at the Friday Harbor Laboratories for help with confocal microscopy. In addition we thank A.O.D. Willows for providing research space at the Friday Harbor Laboratories. This work was supported by an NSF Graduate Student Research Fellowship to M.J.B., a UNC Graduate School Pogue Fellowship to M.J.B. and a Friday Harbor Labs Wainwright Fellowship to M.J.B.

References

Agersborg HPK (1922) Notes on the locomotion of the nudibranchiate mollusk *Dendronotus giganteus* (O'Donoghue). Biol Bull 42:257–266.

Agersborg HPK (1923) The morphology of the nudibranchiate mollusk *Melibe* (syn. Chioraera) *leonina* (Gould). Quart J Microsc Sci 67:507–592.

Audesirk G (1978) Central neuronal control of cilia in *Tritonia diomedea*. Nature 272:541–543.

Beck JC, Cooper MS, Willows AOD (2000) Immunocytochemical localization of pedal peptide in the central nervous system of the gastropod mollusc *Tritonia diomedea*. J Comp Neurol 425:1–9.

Boyle MB, Cohen LB, Macagno ER, Orbach H (1983) The number and size of neurons in the CNS of gastropod molluscs and their suitability for optical recording of activity. Brain Res 226:305–317.

Breidbach O, Kutsch W (1995) Introductory remarks. In: The Nervous System of Invertebrates: An Evolutionary and Comparative Approach (Breidbach O, Kutsch W, eds), pp 1–6. Basel: Birkhauser Verlag.

Bulloch AGM, Ridgeway RL (1995) Comparative aspects of gastropod neurobiology. In: The Nervous System of Invertebrates: An Evolutionary and Comparative Approach (Breidbach O, Kutsch W, eds), pp 89–113. Basel: Birkhauser Verlag.

Cain SD, Wang JH, Lohmann KJ (2006) Immunochemical and electrophysiological analyses of magnetically responsive neurons in the mollusc *Tritonia diomedea*. J Comp Phys A 192:235–245.

Copeland M (1919) Locomotion in two species of the gastropod genus *Alection* with observations on the behavior of pedal cilia. Biol Bull 37:126–138.

Copeland M (1922) Ciliary and muscular locomotion in the gastropod genus *Polinices*. Biol Bull 42:132–142.

Croll RP (1987) Identified neurons and cellular homologues. In: Nervous Systems in Invertebrates (Ali MA, ed), pp 41–59. New York: Plenum Press.

Croll RP, Boudko DY, Hadfield MG (2001) Histochemical survey of transmitters in the central ganglia of the gastropod mollusc *Phestilla sibogae*. Cell Tissue Res 305:417–432.

Crow T, Tian L (2003) Interneuronal projections to identified cilia-activating pedal neurons in *Hermissenda*. J Neurophysiol 89:2420–2429.

Espinoza SY, Breen L, Varghese N, Faulkes Z (2006) Loss of escaped-related giant neurons in a spiny lobster, *Panulirus argus*. Biol Bull:223–231.

Faulkes Z, Paul DH (1997) A map of distal leg motor neurons in the thoracic ganglia of four decapod crustacean species. Brain Behav Evol 49:162–178.

Felsenstein J (1985) Phylogenies and the comparative method. Am Nat 125:1–15.

Garland T Jr, Dickerman AW, Janis CM, Jones JA (1993) Phylogenetic analysis of covariance by computer simulation. Syst Biol 42:265–292.

Garland T Jr, Harvey PH, Ives AR (1992) Procedures for the analysis of comparative data using phylogenetically independent contrasts. Syst Biol 41:18–32.

Gillette R (1991) On the significance of neuronal giantism in gastropods. Biol Bull 180:234–240.

Grafen A (1989) The phylogenetic regression. Phil Trans R Soc Lond B 326:119–157.

Harvey PH, Pagel MD (1991) The Comparative Method in Evolutionary Biology. New York: Oxford University Press.

Katz PS, Harris-Warrick RM (1999) The evolution of neuronal circuits underlying species-specific behavior. Curr Opin Neurobiol 9: 628–633.

Katz PS, Fickbohm DJT, Lynn-Bullock CP (2001) Evidence that the central pattern generator for swimming in *Tritonia* arose from a non-rhythmic neuromodulatory arousal system: Implications for the evolution of specialized behavior. Am Zool 41:962–975.

Lloyd PE, Phares GA, Phillips NE, Willows AOD (1996) Purification and sequencing of neuropeptides from identified neurons in the marine mollusc, *Tritonia*. Peptides 17:17–23.

Lohmann KJ, Willows AOD, Pinter RB (1991) An identifiable molluscan neuron responds to changes in earth-strength magnetic fields. J Exp Biol 161:1–24.

Maddison WP, Maddison DR (2005) Mesquite: A modular system for evolutionary analysis. Version 1.06. http://mesquiteproject.org.

Marois R, Carew T J (1997) Ontogeny of serotonergic neurons in *Aplysia californica*. J Comp Neurol 386:477–490.

Midford PE, Garland T Jr, Maddison WP (2003) PDAP Package.

Moroz LL, Sudlow LC, Jing J, Gillette R (1997) Serotonin-immunoreactivity in peripheral tissues of the opisthobranch mollusks *Pleurobranchaea californica* and *Tritonia diomedea*. J Comp Neurol 382:176–188.

Newcomb JM, Fickbohm DJ, Katz PS (2006) Comparative mapping of serotonin-immunoreactive neurons in the central nervous systems of nudibranch mollusks. J Comp Neurol 499:485–505.

Nusbaum MP, Kristan WB Jr (1986) Swim initiation in the leech by serotonin-containing interneurons, cells 21 and 61. J Exp Biol 122: 277–302.

Page LR, Parries SC (2000) Comparative study of the apical ganglion in planktotrophic caenogastropod larvae: ultrastructure and immunoreactivity to serotonin. J Comp Neurol 418:383–401.

Page LR (2002) Comparative structure of the larval apical sensory organ in gastropods and hypotheses about function and developmental evolution. Invertebr Repro Dev 41:193–200.

Pagel MD (1992) A method for the analysis of comparative data. J Theor Biol 156:431–442.

Paul D (1991) Pedigrees of neurobehavioral circuits: tracing the evolution of novel behaviors by comparing motor patterns, muscles, and neurons in members of related taxa. Brain Behav Evol 38:226–239.

Popescu IR, Willows AOD (1999) Sources of magnetic sensory input to identified neurons active during crawling in the marine mollusc *Tritonia diomedea*. J Exp Biol 202: 3029–3036.

Popescu IR, Frost WN (2002) Highly dissimilar behaviors mediated by a multifunctional network in the marine mollusk *Tritonia diomedea*. J Neurosci 22:1985–1993.

Roth VL (1984) On homology. Biol J Linn Soc 22: 13–29.

Tierney AJ, Godleski MS, Rattananont P (1999) Serotonin-like immunoreactivity in the stomatogastric nervous systems of crayfishes from four genera. Cell Tissue Res 295:537–551.

Turrigiano GG, Selverston AI (1991) Distribution of cholecystokinin-like immunoreactivity within the stomatogastric nervous systems of four species of decapod crustacea. J Comp Neurol 305:164–176.

Wägele H, Willan RC (2000) Phylogeny of the nudibranchia. Zool J Linn Soc-Lond 130:83–181.

Wang JH, Cain SD, Lohmann KJ (2003) Identification of magnetically responsive neurons in the marine mollusc *Tritonia diomedea*. J Exp Biol 206:381–388.

Watson WH, Willows AOD (1992) Evidence for homologous peptidergic neurons in the buccal ganglia of diverse nudibranch mollusks. J Neurobiol 23:173–186.

Weiss KR, Kupfermann I (1976) Homology of the giant serotonergic neurons (metacerebral cells) in *Aplysia* and pulmonate molluscs. Brain Res 117:33–49.

Willows AOD, Dorsett DA, Hoyle G (1973) The neuronal basis of behavior in *Tritonia*. I. Functional organization of the central nervous system. J Neurobiol 4:207–237.

Willows AOD, Pavlova GA, Phillips NE (1997) Modulation of ciliary beat frequency by neuropeptides from identified molluscan neurons. J Exp Biol 200:1433–1439.

Witten JL, Truman JW (1998) Distribution of GABA-like immunoreactive neurons in insects suggests lineage homology. J Comp Neurol 398:515–528.

Wollscheid-Lengeling E, Boore J, Brown W, Wägele H (2001) The phylogeny of Nudibranchia (Opisthobranchia, Gastropoda, Mollusca) reconstructed by three molecular markers. Org Divers Evol 1:241–256.

Wright WG, Kirschman D, Rozen D, Maynard B (1996) Phylogenetic analysis of learning-related neuromodulation in molluscan mechanosensory neurons. Evolution 50:2248–2263.